Cumhuriyet Sci. J., 45(1) (2024) 117-124
DOI: https://doi.org/10.17776/csj.1385759

Cumhuriyet Science Journal

| csj.cumhuriyet.edu.tr | Founded: 2002 ISSN: 2587-2680 e-ISSN: 2587-246X Publisher: Sivas Cumhuriyet University

Dynamics of a Conformable Fractional Order Generalized Richards Growth Model on Star Network with N=20 Nodes

Neriman Kartal [1,a,*]

[1] Deparment of Travel Tourism and Entertainment, Ürgüp Sebahat ve Erol TOKSÖZ Tourism Vocational High School, Nevsehir Hacı Bektas Veli University, Nevsehir, Türkiye.
*Corresponding author

Research Article

History
Received: 03/11/2023
Accepted: 22/02/2024

ABSTRACT

In this study, we analyze dynamical behavior of the conformable fractional order Richards growth model. Before examining the analysis of the dynamical behavior of the fractional continuous time model, the model is reduced to the system of difference equations via utilizing piecewise constant functions. An algebraic condition that ensures the stability of the positive fixed point of the system is obtained. With the center manifold theory, the existence of a Neimark-Sacker bifurcation at the fixed point of the discrete-time system is proven and the direction of this bifurcation is determined. In addition, the discrete dynamical system is also studied on the star network with $N = 20$ nodes. Analysis complex dynamics of Richards growth model into coupled dynamical network shows that the complex star network with $N = 20$ nodes also exhibits Neimark-Sacker bifurcation about the fixed point concerning with parameter c. Numerical simulations are performed to demonstrate the stability, bifurcations and dynamic transition of the coupled network.

Keywords: Fractional order model, Star network, Discrete system, Stability, Neimark-Sacker bifurcation.

[a] nerimangok@nevsehir.edu.tr https://orcid.org/0000-0003-1100-0949

Introduction

In order to describe physical or biological processes many different types of mathematical models such us Malthus, Logistic, Von Bertalanffy, Richards, Gompertz, Blumberg and Turner are used. The most commonly used of these are the logistic and Richards models. Compared with the logistic equation, Richards equations define for more flexible curves of the S shape where the growth curve is asymmetrical and it can define changes in the initial growth stage, rapid growth stage, and stable growth stage of populations. In the literature, there are many successful applications of the Richards growth model in fields such as forest modelers [1], geology [2], COVİD 19 [3,4], Ebola [5], fruit weight [6], microbial growth [7], interaction two-species population [8], traffic [9] and tree growth model [10].

The Richards differential equation has the following form:

$$\frac{dN(t)}{dt} = rN(t)\left(1 - \left(\frac{N(t)}{K}\right)^{\beta}\right). \quad (1)$$

The more general form of the Richards model, called the generalized Richards growth model, is given as follows.

$$\frac{dN(t)}{dt} = rN^{p}(t)\left(1 - \left(\frac{N(t)}{K}\right)^{\beta}\right), \quad (2)$$

where r is the maximum intrinsic rate of increase of N, K is the upper asymptote of N and β is an additional parameter in the Richards equation introduced as a power law so that it can define asymmetric curves and p is known as the deceleration of growth parameter which captures different early stages of the epidemic.

In recent years, the increasing popularity of fractional order derivatives has led to the increase of using fractional order dynamical systems in literature. Many biological and physical processes are successfully modeled in fields such as biology [11], physics [12], chemistry [13] and complex network [14]. The most important advantage of fractional order differential equations over ordinary differential equations is that they can reflect the long memory and hereditary properties of the systems. There are several kinds of definitions for fractional derivatives such as Caputo-Riemann-Liouville and conformable fractional derivatives. Conformal fractional order derivative has many advantages over other fractional order definitions in practice because it reflects many of the properties which already exist in ordinary differential equations.

For all $t > 0$, $\alpha \in (0,1)$, conformable fractional derivative of $f: [0,\infty) \to R$ is defined by

$$(T_{\alpha}f)(t) = \lim_{\varepsilon \to 0} \frac{f(t+\varepsilon t^{1-\alpha}) - f(t)}{\varepsilon} \quad (3)$$

which has the following properties:

$$(T_{\alpha}^{a}f)(t) = (t-a)^{1-\alpha}f'(t), .., \left({}_{\alpha}^{b}Tf\right)(t) = -(b-t)^{1-\alpha}f'(t), \quad (4)$$

where $(T_{\alpha}^{a}f)(t)$ and $\left({}_{\alpha}^{b}Tf\right)(t)$ are the left and right conformable fractional derivative respectively [15-16].

Busenberg and Cooke [17] introduced a new type of differential equations that is called differential equation with piecewise constant arguments in the early 1980s. Since these equations contain both differential equations and difference equations, they have some advantages in applications. In particular, the ability to easily transition from these equations to difference equations is extremely important for population dynamics. In this way, many mathematical models for population dynamics that can describe rich dynamic behaviors such as chaos have been created in the literature [18-21].

Complex network is a type of mathematical graph and examines relationships between objects using connectivity. The objects and connectivity are represented nodes and edges respectively and each node is demonstrated by a nonlinear dynamical system in a complex network. Networks are named according to the shape of the connections such as globally coupled network, star network, Erdos-Renyi network and are used to understand the origin and complexity of the dynamical system. Studying on dynamical analysis of different types of complex networks can be found in the studies [22-27].

In study [28], ElRaheem and Salman consider the Caputo fractional-order Logistic differential equation with piecewise constant arguments given by

$$D^{\alpha}N(t)=\rho x\left(\left[\!\left[\frac{t}{h}\right]\!\right]h\right)\left(1-x\left(\left[\!\left[\frac{t-h}{h}\right]\!\right]h\right)\right),\quad x(0)=x_0\,. \quad (5)$$

Discretization process gives the system of difference equations as follows:

$$\begin{cases} x(n+1)=x(n)+\rho x(n)\big(1-y(n)\big)\frac{h^{\alpha}}{\Gamma(\alpha+1)} \\ y(n+1)=x(n). \end{cases} \quad (6)$$

The conformable fractional-order delay Richards growth model can be defined as follows:

$$T^{\alpha}N(t)=rN^{p}(t)\left(1-\left(\frac{N(t-\tau)}{K}\right)^{\beta}\right). \quad (7)$$

If the piecewise constant arguments are used in the place of the term $t-\tau(t)$ as $\left[\!\left[\frac{t-h}{h}\right]\!\right]$ we obtain

$$T^{\alpha}N(t)=rN^{p}\left(\left[\!\left[\frac{t-h}{h}\right]\!\right]h\right)\left(1-\left(\frac{N\left(\left[\!\left[\frac{t-h}{h}\right]\!\right]h\right)}{K}\right)^{\beta}\right), \quad (8)$$

with the initial condition $N(0)=N_0$ where $N(t)$ is a value of a measure of size or density of an organism or population, β is additional shape parameter, p is deceleration of growth parameter, K is the carrying capacity, $[\![t]\!]$ denotes the integer part of $t\in[0,\infty)$ and h is discretization parameter.

The purpose of this study is to examine stability and bifurcation analysis of the conformable fractional order generalized Richards growth model (8).

Local Stability Analysis

We will first apply a discretization procedure to obtain a system of difference equations from the model (8). Let $t\in[0,\infty)$, $n=0,1,2,\dots$. From property (4) one can obtain

$$(t-nh)^{1-\alpha}\frac{dN(t)}{dt}=rN^{p}(nh-h)\left(1-\left(\frac{N(nh-h)}{K}\right)^{\beta}\right) \quad (9)$$

that gives

$$dN(t)=rN^{p}(nh-h)\left(1-\left(\frac{N(nh-h)}{K}\right)^{\beta}\right)(t-nh)^{\alpha-1}dt. \quad (10)$$

By integrating equation (10) with respect to t on $[nh,t)$, one can hold

$$N(t)-N(nh)=rN^{p}(nh-h)\left(1-\left(\frac{N(nh-h)}{K}\right)^{\beta}\right)\frac{(t-nh)^{\alpha}}{\alpha}. \quad (11)$$

Let $t\to(n+1)h$ in equation (11) and obtain

$$N\big((n+1)h\big)-N(nh)=$$
$$rN^{p}\big((n-1)h\big)\left(1-\left(\frac{N\big((n-1)h\big)}{K}\right)^{\beta}\right)\frac{h^{\alpha}}{\alpha}. \quad (12)$$

To use a suitable notation for the representation of difference equations, we replacing $N(nh)$ by $N(n)$.

$$N(n+1)=N(n)+rN^{p}(n-1)\left(1-\left(\frac{N(n-1)}{K}\right)^{\beta}\right)\frac{h^{\alpha}}{\alpha} \quad (13)$$

If we introduce $x(n)=N(n)$ and $y(n)=N(n-1)$, then we have

$$\begin{cases} x(n+1)=x(n)+r(y(n))^{p}\left(1-\left(\frac{y(n)}{K}\right)^{\beta}\right)\frac{h^{\alpha}}{\alpha} \\ y(n+1)=x(n). \end{cases} \quad (14)$$

Now, we can deal with the stability of the fixed points of model (14). We note that the positive fixed point of the model (14) is $(x^*,y^*)=(K,K)$. Necessary and sufficient algebraic conditions that ensuring the local asymptotic stability of the positive fixed point of the model (14) will be given in the following theorem.

Theorem 1. The fixed point $(x^*,y^*)=(K,K)$ of system (14) is local asymptotically stable if and only if

$$0<r<\frac{\alpha}{h^{\alpha}K^{-1+p}\beta}\,. \quad (15)$$

Proof 1. The Jacobian matrix calculated at positive fixed point $(x^*,y^*)=(K,K)$ of system (14) is

$$J=\begin{pmatrix}1 & -\frac{h^{\alpha}K^{-1+p}r\beta}{\alpha} \\ 1 & 0\end{pmatrix}$$

and the corresponding characteristic equation is

$$\lambda^2+p_1\lambda+p_2=0 \quad (16)$$

where

$$p_1=-1 \quad (17)$$

and

$$p_2=\frac{h^{\alpha}K^{-1+p}r\beta}{\alpha}\,. \quad (18)$$

The following conditions that are called Schur-Cohn criterions can be used for the determining asymptotic stability conditions of the fixed point (x^*,y^*) of the system (14).

i) $1+p_1+p_2>0$

ii) $1-p_1+p_2>0$

iii) $1-p_2>0$

From i) and ii), we have

$$1+p_1+p_2=\frac{h^{\alpha}K^{-1+p}r\beta}{\alpha}>0$$

and

$$1-p_1+p_2=2+\frac{h^{\alpha}K^{-1+p}r\beta}{\alpha}>0,$$

respectively. Under the condition $r < \frac{\alpha}{h^{\alpha}K^{-1+p}\beta}$, we hold

$$1 - p_2 = 1 - \frac{h^{\alpha}K^{-1+p}r\beta}{\alpha} > 0$$

This completes our proof.

Now we give the topological classification of the fixed point of the model (14).

Theorem 2. Assume that $K > 0$. For the fixed point $(x^*, y^*) = (K, K)$, the following topological classification holds:

i) The fixed point is sink if $r < \frac{\alpha}{h^{\alpha}K^{-1+p}\beta}$.

ii) The fixed point is source if $r > \frac{\alpha}{h^{\alpha}K^{-1+p}\beta}$.

iii) The fixed point is a non-hyperbolic if $r = \frac{\alpha}{h^{\alpha}K^{-1+p}\beta}$.

Neimark Sacker Bifurcation Analysis

In this section, we examine the existence and direction of Neimark-Sacker bifurcation about the positive fixed point for the discrete system (14) in line with the studies [29-31].

Theorem 3: System (14) undergoes Neimark-Sacker bifurcation at the fixed point $(x^*, y^*) = (K, K)$. Moreover, if k < 0 then an attracting invariant cycle will appear for $r > r^*$, if k > 0 then a repelling invariant cycle will appear for $0 < r < r^*$.

Proof 2. From the characteristic equation of the linearized system at the positive fixed point, the eigenvalues can be calculated as follows.

$$\lambda_{1,2} = \frac{1}{2} \pm i\frac{\sqrt{K\alpha(4h^{\alpha}K^{p}r\beta - K\alpha)}}{2K\alpha}. \tag{19}$$

From the solution of equation $1 - p_2 = 0$ in accordance with parameter r gives the Neimark-Sacker bifurcation point as follows:

$$r = r^* = \frac{\alpha}{h^{\alpha}K^{-1+p}\beta}. \tag{20}$$

For $r = r^*$, these eigenvalues leads to

$$|\lambda_{1,2}| = \left|\frac{1}{2} \pm \frac{i\sqrt{3}}{2}\right| = |a \pm ib| = 1.$$

The transversality condition

$$\frac{d|\lambda_{1,2}(r)|}{dr}\Big|_{r=r^*} = \frac{h^{\alpha}K^{-1+p}\beta}{2\alpha} \neq 0 \tag{21}$$

is always satisfied for all parameter values. In addition, non-resonance conditions is always satisfied for $p_1 \neq 0,1$.

Let $u = x - x^*$ and $v = y - y^*$, then the system (14) is transformed into

$$\begin{pmatrix} u \\ v \end{pmatrix} \to \begin{pmatrix} 1 & -1 \\ 1 & 0 \end{pmatrix}\begin{pmatrix} u \\ v \end{pmatrix} + \begin{pmatrix} f_1(u,v) \\ f_2(u,v) \end{pmatrix} \tag{22}$$

where

$$f_1(u,v) = m_{13}u^2 + m_{14}uv + m_{15}v^2 + m_{16}u^3 + m_{17}u^2v + m_{18}uv^2 + m_{19}v^3 + O((|u| + |v|)^4)$$
$$f_2(u,v) = m_{23}u^2 + m_{24}uv + m_{25}v^2 + m_{26}u^3 + m_{27}u^2v + m_{28}uv^2 + m_{29}v^3 + O((|u| + |v|)^4)$$

and

$$m_{13} = m_{14} = m_{16} = m_{17} = m_{18} = m_{23} = m_{24} = m_{25} = m_{26} = m_{27} = m_{28} = m_{29} = 0$$
$$m_{15} = -\frac{-1 + 2p + \beta}{2K}$$
$$m_{19} = -\frac{2 + 3(-2+p)p - 3\beta + 3p\beta + \beta^2}{6K^2}.$$

By using transformation $\begin{pmatrix} u \\ v \end{pmatrix} = T\begin{pmatrix} X \\ Y \end{pmatrix}$, then the map (22) rewritten as the following form

$$\begin{pmatrix} X \\ Y \end{pmatrix} \to \begin{pmatrix} a & -b \\ b & a \end{pmatrix}\begin{pmatrix} X \\ Y \end{pmatrix} + \begin{pmatrix} F_1(X,Y) \\ F_2(X,Y) \end{pmatrix} \tag{23}$$

where

$$T = \begin{pmatrix} \frac{\sqrt{3}}{2} & \frac{1}{2} \\ 0 & 1 \end{pmatrix}$$
$$F_1(X,Y) = -\frac{Y^2(-1+2p+\beta)}{\sqrt{3}K} - \frac{Y^3(2 - 6p + 3p^2 - 3\beta + 3p\beta + \beta^2)}{3\sqrt{3}K^2} + O((|u| + |v|)^4)$$
$$F_2(X,Y) = 0.$$

The constant k, which will determine the direction of the Neimark-Sacker bifurcation, can be calculated using the following equation.

$$k = -\text{Re}\left[\frac{(1-2\lambda)\bar{\lambda}^2}{1-\lambda}\xi_{11}\xi_{20}\right] - \frac{1}{2}|\xi_{11}|^2 - |\xi_{02}|^2 + \text{Re}[\bar{\lambda}\xi_{21}] = \frac{2p-5p^2+\beta-5p\beta-\beta^2}{16K^2} \qquad (24)$$

where

$$\xi_{20} = \frac{1}{8}\left((F_{1XX} - F_{1YY} + 2F_{2XY}) + i(F_{2XX} - F_{2YY} - 2F_{1XY})\right) = \frac{-1+2p+\beta}{4\sqrt{3}K}$$

$$\xi_{11} = \frac{1}{4}\left((F_{1XX} + F_{1YY}) + i(F_{2XX} + F_{2YY})\right) = -\frac{-1+2p+\beta}{2\sqrt{3}K}$$

$$\xi_{02} = \frac{1}{8}\left((F_{1XX} - F_{1YY} - 2F_{2XY}) + i(F_{2XX} - F_{2YY} + 2F_{1XY})\right) = \frac{-1+2p+\beta}{4\sqrt{3}K}$$

$$\xi_{21} = \frac{1}{16}\left((F_{1XXX} + F_{1XYY} + F_{2XXY} + F_{2YYY}) + i(F_{2XXX} + F_{2XYY} - F_{1XXY} - F_{1YYY})\right) = \frac{i(2+3p^2+3p(-2+\beta)-3\beta+\beta^2)}{8\sqrt{3}K^2}.$$

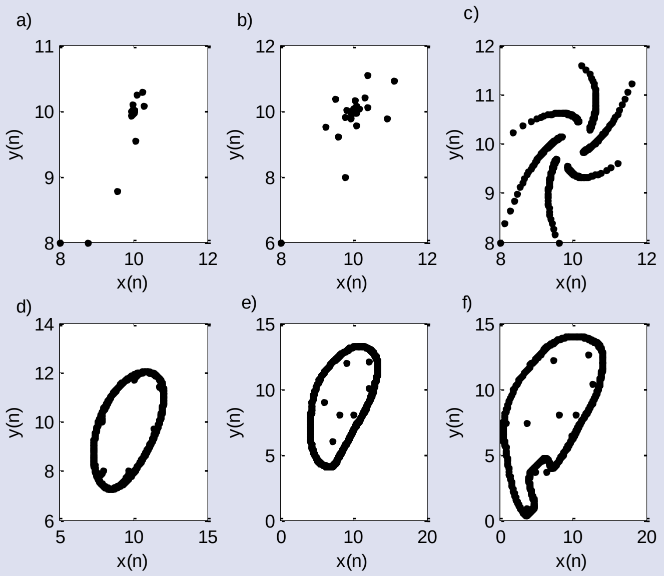

Figure 1. Phase portraits of the discrete model (14) with respect to parameter r for $r = 1$ (a), $r = 1.5$ (b), $r = 2.08295$ (c), $r = 2.3$ (d) $r = 2.6$ (e), $r = 3$ (f) where α=0.95, β=0.7, K=10, h=0.5, p=1.1, x(1)=y(1)=7.

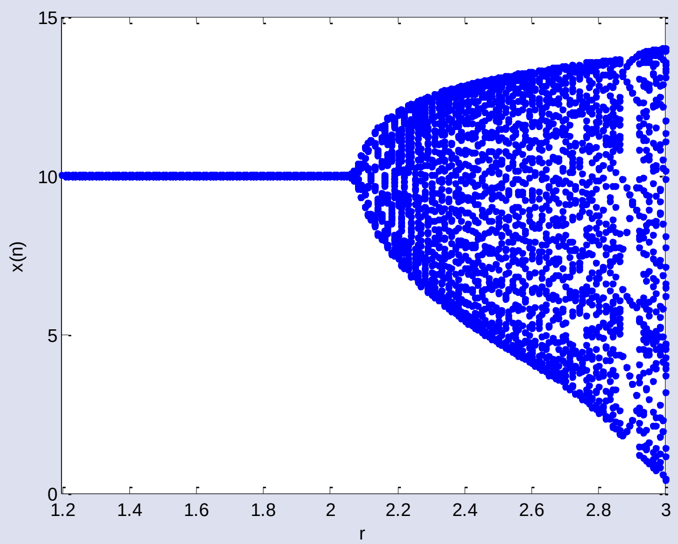

Figure 2. Bifurcation diagram of the discrete system (14) in accordance with parameter r, where $\alpha = 0.95, \beta = 0.7, K = 10,\ h = 0.5, p = 1.1, x(1) = y(1) = 7$.

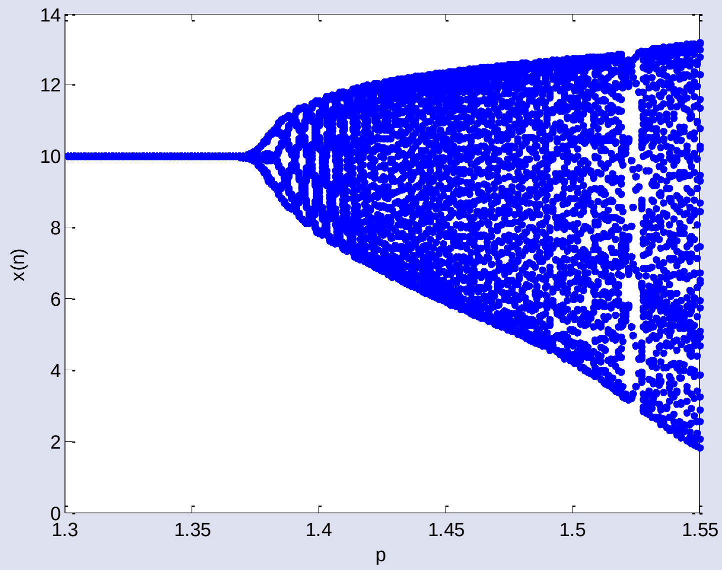

Figure 3. Bifurcation diagram of the discrete system (14) in accordance with parameter p, where $\alpha = 0.95, \beta = 0.7, K = 10,\ h = 0.5, r = 1.1, x(1) = y(1) = 7.$

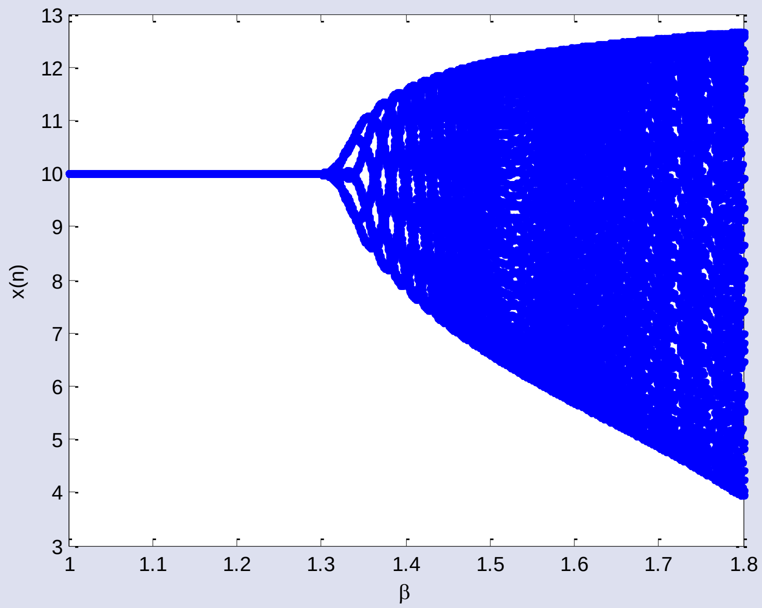

Figure 4. Bifurcation diagram of the discrete system (14) in accordance with parameter β, where $\alpha = 0.95, p = 1.1, K = 10,\ h = 0.5, r = 1.1, x(1) = y(1) = 7.$

Dynamical Analysis of the model on Star Network

Taking into account a dynamical network consisting of N linearly and diffusively coupled nodes, with each node describe a two-dimensional dynamical system defined by discrete system (14). Let's consider the equation (14) as the following form:

$$\begin{cases} x(k+1) = x(k) + r(y(k))^p \left(1 - \left(\frac{y(k)}{K}\right)^\beta\right)\frac{h^\alpha}{\alpha} = f\big(x(k), y(k)\big) \\ y(k+1) = x(k) = g\big(x(k), y(k)\big). \end{cases} \tag{25}$$

This dynamical network is defined by

$$\begin{cases} x_i(k+1) = f\big(x_i(k), y_i(k)\big) - c\sum_{j=1}^{N} a_{ij} f\Big(x_j(k), y_j(k)\Big) \\ y_i(k+1) = g\big(x_i(k), y_i(k)\big) - c\sum_{j=1}^{N} a_{ij} g\Big(x_j(k), y_j(k)\Big), \end{cases} \tag{26}$$

where i and j are the sequence number of the nodes and c describes the coupling strength of the network. The coupling matrix $A \in R^{NxN}$ can be expressed by

$$A = \begin{pmatrix} d_{11} & a_{12} & a_{13} & \cdots & a_{1N} \\ a_{12} & d_{22} & a_{23} & \cdots & a_{2N} \\ a_{13} & a_{23} & d_{33} & \cdots & a_{3N} \\ \vdots & \vdots & \vdots & \ddots & \ldots \\ a_{1N} & a_{2N} & a_{3N} & \cdots & d_{NN} \end{pmatrix} \tag{27}$$

If there is a connection between node i and j, then $a_{ij} = 1$; otherwise, $a_{ij} = 0$ $(i \neq j)$. Let $a_{ii} = d_i$, $i = 1,2, \ldots N$, where d_i is the degree of node i and can be defined as

$$d_{ii} = -\sum_{j=1, j\neq i}^{N} a_{ij} = -\sum_{j=1, j\neq i}^{N} a_{ji}$$

The system (26) can be written in matrix form as follows:

$$\begin{cases} X_{k+1} = (I - cA) f\big(X(k), Y(k)\big) \\ Y_{k+1} = (I - cA) g\big(X(k), Y(k)\big) \end{cases} \tag{28}$$

where $X_k = \big(x_1(k), x_2(k), \ldots . x_N(k)\big)$, $Y_k = \big(y_1(k), y_2(k), \ldots . y_N(k)\big)$ and $I \in R^{NXN}$ identity matrix.

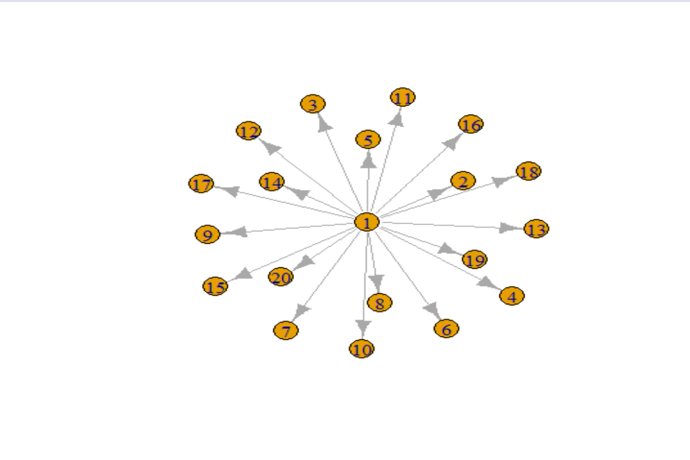

Figure 5. Star network with N = 20 nodes.

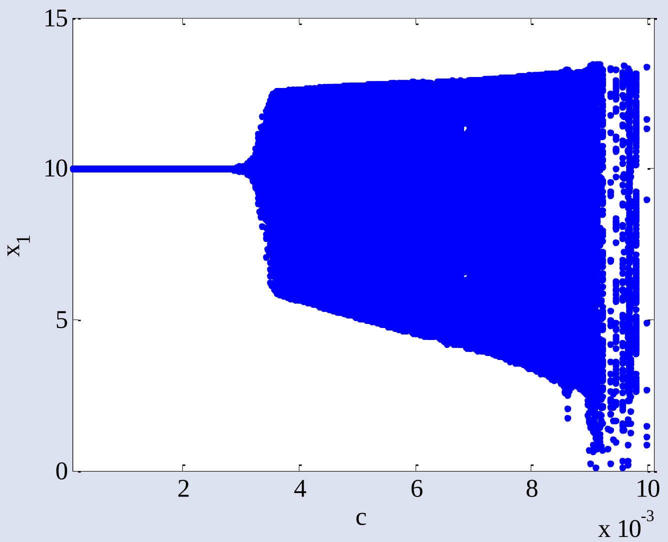

Figure 6. Neimark-Sacker bifurcation in the star network in accordance with parameter c, where α = 0.95, β = 0.7, p = 1.1, K = 10, h = 0.5, r = 2.07 and N = 20.

Result and Discussion

In this study, we consider the conformable fractional order Richards growth model with piecewise constant arguments. Adding piecewise constant arguments to the model (7) make it possible to transition to the system of difference equation (14). The positive fixed point of the system (14) is obtained as $(x^*,\ y^*) = (K, K)$ and its stability condition is given in equation (15). To test this algebraic condition based on changing the growth rate parameter r of the population, we select the parameter values as $\alpha = 0.95, \beta = 0.7, K = 10,\ h = 0.5, p = 1.1$ and $x(1) = y(1) = 7$. The stability region according to the change of the parameter r is obtained as $r < 2.08295$. It can be easily seen in the Figure 1a and 1b that, the fixed point (10,10) of the system (14) is local asymptotically stable.

In bifurcation analysis, we deal with the existence and direction of the Neimark-Sacker bifurcation about the positive fixed point of the system (14). From the solutions of the equation $1 - p_0 = 0$ with respect tom parameter r, the eigenvalue assignment condition can be obtained as $r^* = \frac{\alpha}{h^\alpha K^{-1+p}\beta}$. In addition From the equation (21) and the conditions $p_1 \neq 0{,}1$, transversality and non-resonance conditions are always satisfied for all of the positive parameter values. Now, all of the conditions for the existence of the Neimark-Sacker bifurcation are satisfied and this bifurcation is shown in Figure 1c and Figure 2. From the equation (24), the value of k that determines the direction of the Neimark-Sacker bifurcation is calculated as $k = -0.00468125$ which show the existence of supercritical Neimark-Sacker bifurcation. We also deal with the bifurcation analysis for the other parameters such as β and p. The effect of the deceleration of growth parameter p and additional shape parameter β on the dynamic structure of the system is seen in Figures 3 and Figure 4, respectively. From these figures we can also observe the Neimark-Sacker bifurcation for the parameter values $p^* = 1.37721$ and $\beta^* = 1.32529$ and so the model exhibits more unstable dynamics behavior for increased parameters p and β.

Model (12) and model (6) exhibit similar dynamic behaviors such as Neimark-Sacker bifurcation and chaos according to changing the growth rate parameter r and ρ. However, model (12) is a more generalized version of model (6) and includes extra parameters such as β and p. We provide that model (12) also exhibits Neimark-Sacker bifurcation according to changing parameters β and p.

Discrete dynamical system (14) is also considered on the star network with $N = 20$ nodes. In order to investigate the complex dynamics of the model (14) into coupled dynamical network, system (26) is represented the state equations of star network. All simulations have used the same initial condition for all nodes, which are slightly different from the fixed point. Figure 5 shows the star network with $N = 20$ nodes. For the star network with $N = 20$ nodes, the coupling matrix A can be obtained from the equation (27) as follows.

$$A = \begin{pmatrix}
-19 & 1 & 1 & 1 & 1 & 1 & 1 & 1 & 1 & 1 & 1 & 1 & 1 & 1 & 1 & 1 & 1 & 1 & 1 & 1 \\
1 & -1 & 0 & 0 & 0 & 0 & 0 & 0 & 0 & 0 & 0 & 0 & 0 & 0 & 0 & 0 & 0 & 0 & 0 & 0 \\
1 & 0 & -1 & 0 & 0 & 0 & 0 & 0 & 0 & 0 & 0 & 0 & 0 & 0 & 0 & 0 & 0 & 0 & 0 & 0 \\
1 & 0 & 0 & -1 & 0 & 0 & 0 & 0 & 0 & 0 & 0 & 0 & 0 & 0 & 0 & 0 & 0 & 0 & 0 & 0 \\
1 & 0 & 0 & 0 & -1 & 0 & 0 & 0 & 0 & 0 & 0 & 0 & 0 & 0 & 0 & 0 & 0 & 0 & 0 & 0 \\
1 & 0 & 0 & 0 & 0 & -1 & 0 & 0 & 0 & 0 & 0 & 0 & 0 & 0 & 0 & 0 & 0 & 0 & 0 & 0 \\
1 & 0 & 0 & 0 & 0 & 0 & -1 & 0 & 0 & 0 & 0 & 0 & 0 & 0 & 0 & 0 & 0 & 0 & 0 & 0 \\
1 & 0 & 0 & 0 & 0 & 0 & 0 & -1 & 0 & 0 & 0 & 0 & 0 & 0 & 0 & 0 & 0 & 0 & 0 & 0 \\
1 & 0 & 0 & 0 & 0 & 0 & 0 & 0 & -1 & 0 & 0 & 0 & 0 & 0 & 0 & 0 & 0 & 0 & 0 & 0 \\
1 & 0 & 0 & 0 & 0 & 0 & 0 & 0 & 0 & -1 & 0 & 0 & 0 & 0 & 0 & 0 & 0 & 0 & 0 & 0 \\
1 & 0 & 0 & 0 & 0 & 0 & 0 & 0 & 0 & 0 & -1 & 0 & 0 & 0 & 0 & 0 & 0 & 0 & 0 & 0 \\
1 & 0 & 0 & 0 & 0 & 0 & 0 & 0 & 0 & 0 & 0 & -1 & 0 & 0 & 0 & 0 & 0 & 0 & 0 & 0 \\
1 & 0 & 0 & 0 & 0 & 0 & 0 & 0 & 0 & 0 & 0 & 0 & -1 & 0 & 0 & 0 & 0 & 0 & 0 & 0 \\
1 & 0 & 0 & 0 & 0 & 0 & 0 & 0 & 0 & 0 & 0 & 0 & 0 & -1 & 0 & 0 & 0 & 0 & 0 & 0 \\
1 & 0 & 0 & 0 & 0 & 0 & 0 & 0 & 0 & 0 & 0 & 0 & 0 & 0 & -1 & 0 & 0 & 0 & 0 & 0 \\
1 & 0 & 0 & 0 & 0 & 0 & 0 & 0 & 0 & 0 & 0 & 0 & 0 & 0 & 0 & -1 & 0 & 0 & 0 & 0 \\
1 & 0 & 0 & 0 & 0 & 0 & 0 & 0 & 0 & 0 & 0 & 0 & 0 & 0 & 0 & 0 & -1 & 0 & 0 & 0 \\
1 & 0 & 0 & 0 & 0 & 0 & 0 & 0 & 0 & 0 & 0 & 0 & 0 & 0 & 0 & 0 & 0 & -1 & 0 & 0 \\
1 & 0 & 0 & 0 & 0 & 0 & 0 & 0 & 0 & 0 & 0 & 0 & 0 & 0 & 0 & 0 & 0 & 0 & -1 & 0 \\
1 & 0 & 0 & 0 & 0 & 0 & 0 & 0 & 0 & 0 & 0 & 0 & 0 & 0 & 0 & 0 & 0 & 0 & 0 & -1
\end{pmatrix}$$

Now let's consider the nodes with the highest degree in the star network with $N = 20$ nodes. which for is 1 and . Figure 6 shows that if the coupling parameter c reaches the some critical value where it is interval $c \in [2x10^{-3}, 4x10^{-3}]$, then Neimark-Sacker bifurcation occurs about the positive fixed point.

Acknowledgments

The authors declare that there is no conflict of interest.

Conflicts of interest

There are no conflicts of interest in this work.

References

[1] Lei Y., Zhang S.Y., Comparison and selection of growth models using the Schnute model, *J. For. Sci*., 52 (2006) 188-196.

[2] Yang Y., Fan W., Long L., Xu Z., Zhao Z., Zhang H., Application of the Richards Model in Settlement Prediction of Loess-Filled Foundations, *Appl. Sci*., 12 (2022) 11350.

[3] Sharon E.A., Aharoni A., Generalized logistic growth modeling of the COVID-19 pandemic in Asia, *Infect. Dis. Model*., 5 (2020) 502e509 .

[4] Zreiq R., Kamela S., Boubaker S., Al-Shammary A., Algahtani F.D., Alshammari F., Generalized Richards model for predicting COVID -19 dynamics i n Saudi Arabia based on particle swarm optimization algorithm, *Public Health*., 7 (2020) 828-843 .

[5] Pell B., Kuang Y., Viboud C., Chowell G., Using phenomenological models for forecasting the 2015 Ebola challenge, *Epidemics*., 22 (2018) 62-70.

[6] Gerhard D., Moltchanova E., A Richards growth model to predict fruit weight, Aust. N. Z. *J. Stat*., 64 (2022) 413-421.

[7] Teleken J.T., Galvao A.C., Robazza W.S., Use of modified Richards model to predict isothermal and non-isothermal microbial growth, Braz. *J. Microbiol*., 49 (2018) 614-620.

[8] Cabella B.C.T., Ribeiro F., Martinez A.S., Effective carrying capacity and analytical solution of a particular case of the Richards-like two-species population dynamics model, *Physica A*., 391 (2012) 1281-1286.

[9] He J., Mao S., Ng A.K.Y., Neural computing for grey Richards differential equation to forecast traffic parameters with various time granularity, *Neurocomputing*., 549 (2023) 126394.

[10] Protazio J.M.B, Souza M.A., Diaz J.C.H., Flores J.G.E., Sanches C.A.P., Parra A.C., Wehenkel C., A Dynamical Model Based on the Chapman–Richards Growth Equation for Fitting Growth Curves for Four Pine Species in Northern Mexico, *Forests*., 13 (2022) 1866.

[11] Magin R.L., Fractional calculus models of complex dynamics in biological tissues, *Comput. Math. with Appl*., 59 (2010) 1586-1593.

[12] Zhou P., Ma J., Tang J., Clarify the physical process for fractional dynamical systems, *Nonlinear Dyn*., 100 (2020) 2353-2364.

[13] Veeresha P., The efficient fractional order based approach to analyze chemical reaction associated with pattern formation, *Chaos. Solit. Fractals*., 165 (2022) 112862.

[14] Singh R., Rehman A.U., Masud M., Alhumyani H.A., Mahajan S., Pandit A.K., Agarwal P., Fractional order modeling and analysis of dynamics of stem cell differentiation in complex network, *AIMS math*., 7 (2022) 5175-5198.

[15] Khalil R., Horani M.A., Yousef A., Sababheh M., A new definition of fractional derivative, *J. Comput. Appl. Math*., 264 (2014) 65-70.

[16] Abdeljawad T., On conformable fractional calculus, *J. Comput. Appl. Math*., 279 (2015) 57-66.

[17] Busenberg S., Cooke K.L., Models of vertically transmitted diseases with sequential continuous dynamics, Nonlinear Phenomena in Mathematical Sciences, Academic Press, New York (1982).

[18] Ozturk I., Bozkurt F., Gurcan F., Stability analysis of a mathematical model in a microcosm with piecewise constant arguments, *Math. Biosci*., 240 (2012) 85-91.

[19] Bozkurt F., Yousef A., Bilgil H., Baleanu D., A mathematical model with piecewise constant arguments of colorectal cancer with chemo-immunotherapy, *Chaos Soliton Fract.,* 168 (2023) 113207.

[20] Gurcan F., Kartal S., Ozturk I., Bozkurt F., Stability and bifurcation analysis of a mathematical model for tumor-immune interaction with piecewise constant arguments of delay, *Chaos Soliton. Fract*., 68 (2014) 169-179.

[21] Kartal S., Gurcan F., Stability and bifurcations analysis of a competition model with piecewise constant arguments, *Math. Methods. Appl. Sci*., 38 (2015) 1855-1866.

[22] Wang Z., Jiang G., Yu W., He W., Cao J., Xiao M., Synchronization of coupled heterogeneous complex networks, *J. Franklin Inst*., 354 (2017) 4102–4125.

[23] Huang T., Zhang H., Ma S., Pan G., Wang Z., Huang H., Bifurcations, complex behaviors, and dynamic transition in a coupled network of discrete predator-prey system, *Discrete Dyn. Nat. Soc*.., 2019 (2019) Article ID 2583730.

[24] Li X., Chen G., Ko K.T., Transition to chaos in complex dynamical networks, *Physica A Stat. Mech. Appl*., 338 (2004) 367–378.

[25] Nepomuceno E.G., Perc M., Computational chaos in complex networks, *J. Complex Netw*., 8 (2020) cnz015.

[26] Ahmed E., Matouk A.E., Complex dynamics of some models of antimicrobial resistance on complex networks, *Math. Methods Appl. Sci*., 44 (2021) 1896-1912

[27] Zhang H.F., Rui X.W, Fu X.C., The emergence of chaos in complex dynamical networks, *Chaos Soliton. Fract*., 28 (2006) 472-479.

[28] El Raheem Z.F., Salman S.M., On a discretization process of fractional-order logistic differential equation, *J. Egypt. Math. Soc*., 22 (2014) 407-412.

[29] Guckenheimer J., Holmes P., Nonlinear Oscillations, Dynamical Systems, and Bifurcations of Vector Fields, Springer, 1983

[30] Kangalgil F., Neimark–sacker bifurcation and stability analysis of a discrete-time prey–predator model with allee effect in prey, *Adv. Differ. Equ*., 92 (2019)

[31] Kangalgil F., Işık S., Controlling chaos and neimark-sacker bifurcation in a discrete-time predator-prey system, *Hacet. J. Math. Stat*., 49 (2020) 1761 – 1776.